Turk Neurosurg, 2024

Original Investigation

DOI: 10.5137/1019-5149.JTN.46251-24.3

Received: 16.01.2024
Accepted: 19.09.2024

Published Online: 18.10.2024

Predictive Value of T2-weighted Perfusion and T1-weighted Permeability MRI Parameters in Determining IDH Mutational Status and Grade of Gliomas

Sabahattin YUZKAN[1], Mehmet KARAGULLE[2], Merve SAM OZDEMIR[2], Samet MUTLU[2], Burak KOCAK[2]

[1]Koc University Hospital, Department of Radiology, Zeytinburnu, Istanbul, Türkiye
[2]University of Health Sciences, Basaksehir Cam and Sakura City Hospital, Department of Radiology, Basaksehir, Istanbul, Türkiye

Corresponding author: Sabahattin YUZKAN ✉ sabahyuzkan@gmail.com

ABSTRACT

AIM: To assess the performance metrics of perfusion and permeability magnetic resonance imaging (MRI) parameters with optimal cut-offs in differentiating isocitrate dehydrogenase (IDH) genotype and tumor grade in patients with grade 2–4 gliomas.

MATERIAL and METHODS: This retrospective study included 36 patients surgically diagnosed with grade 2–4 glioma (six grade 2, seven grade 3, and 23 grade 4) with known IDH genotypes (23 IDH wild-type, 13 IDH mutant) between November 2021 and August 2023. All patients underwent preoperative perfusion and permeability MRI examinations with a 3.0 Tesla scanner. Parameters were calculated on colored map images. Using the intraclass correlation coefficient, intra- and inter-observer agreement was assessed. Following multiple testing correction, the perfusion parameters with statistically significant differences were subjected to receiver operating characteristic (ROC) analysis.

RESULTS: Five MRI parameters (rCBV and rCBF from perfusion; Ktrans, Ve, and Vp from permeability) showed a significant difference between groups in terms of IDH genotype ($p<0.001$). In ROC analysis, the best parameters in differentiating IDH genotype included rCBV and Ktrans; rCBV with a cut-off of 5.58 achieved an area under the ROC curve (AUC), sensitivity, specificity, and accuracy of 0.883, 95.7%, 76.9%, and 88.8%, respectively. For Ktrans, with a cut-off of 0.0727 min^{-1}, these values were 0.893, 100%, 69.2%, and 88.8%, respectively. In ROC analysis, these two parameters with rCBF and Ve also showed good performance in differentiating low- and high-grade gliomas with an AUC, sensitivity, and accuracy exceeding 0.940, 86%, and 88%, respectively.

CONCLUSION: Perfusion and permeability MRI may provide useful parameters in differentiating the IDH genotype and grade of gliomas.

KEYWORDS: Dynamic contrast-enhanced, Dynamic susceptibility contrast, Glioma grading, Isocitrate dehydrogenase, Magnetic resonance imaging

ABBREVIATIONS: DCE-MRI: Dynamic contrast-enhanced magnetic resonance imaging, **DSC-MRI:** Dynamic susceptibility contrast magnetic resonance imaging, **rCBF:** Relative cerebral blood flow, **rCBV:** Relative cerebral blood volume, **AUC:** Area under the receiver operating characteristic curve, **CNS:** Central nervous system, **ICC:** Intraclass correlation, **IDH:** Isocitrate dehydrogenase, **Ktrans:** Volume transfer constant, **Kep:** Reflux transfer rate, **ROC:** Receiver operating characteristic, **SD:** Standard deviation, **WHO:** World Health Organization, **Ve:** Extravascular-extracellular volume fraction, **Vp:** Fractional plasma volume

Sabahattin YUZKAN : 0000-0002-3066-1737
Mehmet KARAGULLE : 0000-0002-1631-8975
Merve SAM OZDEMIR : 0000-0001-6977-2330
Samet MUTLU : 0000-0001-6867-2872
Burak KOCAK : 0000-0002-7307-396X

INTRODUCTION

Gliomas are the most prevalent primary tumors of the central nervous system (CNS) in adults (4). Constituting nearly 70% of all adult brain tumors, gliomas have an annual incidence of six cases per 100,000 individuals (18,22). The newly revised (5th edition) 2021 World Health Organization (WHO) classification of CNS tumors categorizes gliomas into grades 1–4 based on their histopathological features. This classification system has increasingly emphasized the importance of molecular characteristics in glioma subtyping (11).

Prognostic evaluation and treatment planning of gliomas are strongly related to isocitrate dehydrogenase (IDH) mutation status and tumor grade (2,11,26). IDH mutations arise early in the process of carcinogenesis, and patients with IDH mutations tend to have better survival rates than those with IDH wild-type (14,26). Thus, IDH wild-type tumors are classified as high-grade gliomas in the new classification without exception (11,26). Since IDH mutations are correlated with improved prognosis, the potential to predict IDH mutation status prior to surgery may add significant implications for clinical decision-making and surgical management (17,26). Conversely, in clinical practice, determining the IDH mutation status and glioma grade traditionally involves postoperative assessment of histopathological samples obtained through biopsy or surgical excision (7). However, these invasive procedures are unsuitable for patients who cannot undergo surgery. Therefore, a non-invasive method for predicting IDH genotype and tumor grade is urgently required.

Considering the different pathophysiological processes between glioma subtypes and the consequential alterations in glioma vascularity, using perfusion-based imaging techniques could increase the diagnostic accuracy of non-invasive characterization of glioma subtypes. Hence, numerous literature studies have focused on investigating perfusion-based MRI using dynamic susceptibility contrast (DSC), known as T2*-weighted perfusion, or dynamic contrast-enhanced (DCE), also known as T1-weighted permeability, magnetic resonance imaging (MRI) to non-invasively identify the IDH mutation status (16). Nonetheless, a consensus regarding which MRI parameters and cut-offs should be used for prediction has yet to be reached (16). The primary objective of the current study was to quantitatively investigate the diagnostic efficacy of the most commonly used parameters, DSC-MRI [relative cerebral blood volume (rCBV), relative cerebral blood flow (rCBF)] and DCE-MRI [volume transfer constant (Ktrans), extravascular-extracellular volume fraction (Ve), reflux transfer rate (Kep), fractional plasma volume (Vp)], in predicting the IDH mutation status and grade of gliomas.

MATERIAL and METHODS

Ethical Considerations

Ethical approval for the present single-center study was granted by the local ethics committee (protocol code: 2023-17; decision date: 11/01/2023), and the necessity for written informed consent was waived due to its retrospective design.

Study Design

The current study included patients who had received a diagnosis of grade 2–4 glioma with known IDH mutation status and undergone DSC- and DCE-MRI examinations before surgery between November 2021 and August 2023.

The inclusion criteria of the study were as follows: i, patients aged 18 years and above; ii, definitive diagnosis of grade 2–4 glioma; iii, known IDH mutation status according to the 2021 WHO classification (11); and iv, no prior corticosteroid, chemoradiotherapy, or antiangiogenic treatment before MRI examination.

The following criteria determined exclusion: i, patients with a WHO grade 1 glioma diagnosis, since this does not include assessment of IDH mutation status, and ii, MRI scans that were not optimal for assessment for technical reasons, such as vascular access problems during contrast administration or noticeable artifacts hindering diagnostic evaluation. A few glioblastoma cases were selected from the database for our previous study (27).

MRI Acquisition Protocols

All examinations were conducted using a 3.0 Tesla MRI scanner (Ingenia, Philips Healthcare) along with a 32-channel phased-array head coil in the supine position. All MRI scans were performed before the neurosurgical resection or medical therapy.

All MRI examinations included DSC-MRI and DCE-MRI in addition to conventional MRI. First, conventional MRI protocol was completed, including axial spin-echo T1-weighted imaging, transverse T2-weighted imaging, 3D axial T2-weighted fluid-attenuated inversion recovery sequence, susceptibility-weighted imaging, and diffusion-weighted imaging using echo-planar imaging sequences in the axial plane with b = 0 and 1000 s/mm^2. DCE-MRI was then obtained, followed by DSC-MRI examination. DSC-MRI was performed in compliance with recommendations in the consensus statement (5).

DCE-MRI was performed with pre- and post-contrast dynamic gradient-echo T1-weighted sequences [i.e., turbo-field echo (TFE)] using the following parameters: repetition time (TR)/echo time (TE) 3.53/1.67 ms; flip angle 8°; matrix 128 × 125; field of view (FOV) 220 × 220 mm; and section thickness, 3 mm. Fifty dynamic scans were performed with a temporal resolution of 5 s.

DSC-MRI examinations were acquired in the axial plane using a field echo echo-planar imaging sequence (FE-EPI) with the following parameters: TR/TE, 2265/30 ms; flip angle, 75°; matrix, 128 × 128; FOV, 224 × 224 mm; section thickness, 3 mm; and voxel size, 2.33 × 2.39 × 4.00 mm.

For both DCE- and DSC-MRI examinations, a contrast medium (gadolinium-based) was given intravenously in a bolus of 0.1 mmol/kg at a rate of 5 ml/s, with a 20 ml saline flush administered afterwards. The DCE-MRI examination provided a pre-bolus of contrast to mitigate T1 effects caused by contrast leakage during the DSC-MRI.

The selected perfusion imaging parameters were as follows: for DSC-MRI, rCBV and rCBF; for DCE-MRI, Ktrans, Ve, Kep, and Vp.

Image Processing and Analysis

DSC- and DCE-MRI perfusion image datasets were processed using the Philips IntelliSpace Portal to create colored map images of rCBV, rCBF, Ktrans, Ve, Kep, and Vp parameters.

Two neuroradiologists, each with 4 years of experience, independently reviewed all the anonymized MRI data. They were unaware of any clinical details or histopathological results. The radiologists were instructed to use the "hotspot method" by placing a circular region of interest (ROI) within the tumor area that visually appeared mainly hyperperfused on the colored relative CBV and CBF map images. Maximum rCBV and rCBF values were obtained by rating these values to the contralateral normal-appearing centrum semiovale, which is found to be the most reliable reference area (27). Normalized rCBV and rCBF measurements were thus obtained. Absolute values of Ktrans, Ve, Kep, and Vp were then calculated with similar-sized ROIs selected on the highest permeability area of the tumor on the colored map images. All circular ROIs were manually drawn by readers and ranged from 20 to 30 mm^2. By using conventional sequences in ROI analysis, care was taken to avoid cystic, necrotic, and hemorrhagic regions, normal grey matter, and intratumoral non-neoplastic vascular structures that could influence the values. Samples were taken from the solid component in cases where tumor enhancement was present. Figure 1 exemplifies the ROI analysis of a case.

Recorded data encompassed normalized rCBV and rCBF, absolute Ktrans, Ve, Kep, and Vp values, WHO grade, and IDH mutation status, as well as gender and age data.

Statistical Analysis

Jamovi v2.2.5 was used to conduct statistical analysis. The intraclass correlation coefficient (ICC) was estimated based on a two-way model, single measurement, and absolute agreement or consistency to measure intra- and inter-reader reproducibility (10,13). The interpretation scale for the ICC was as follows: <0.5, poor; ≥0.5 and <0.75, moderate; ≥0.75 and <0.9, good; and ≥0.9, excellent (10). The normality of continuous variables was determined using the *Shapiro-Wilk test*. Depending on the statistical data distribution and number of classes, the *Student t-test*, *Mann-Whitney U test*, or *Kruskal-Wallis test (non-parametric one-way analysis of variance)* was used to evaluate statistical differences among continuous variables. Post hoc analysis of the *Kruskal-Wallis test* results was performed according to *Dwass-Steel-Critchlow-Fligner* pairwise comparisons. All multiple comparisons were subjected to multiplicity correction using the *Bonferroni method*

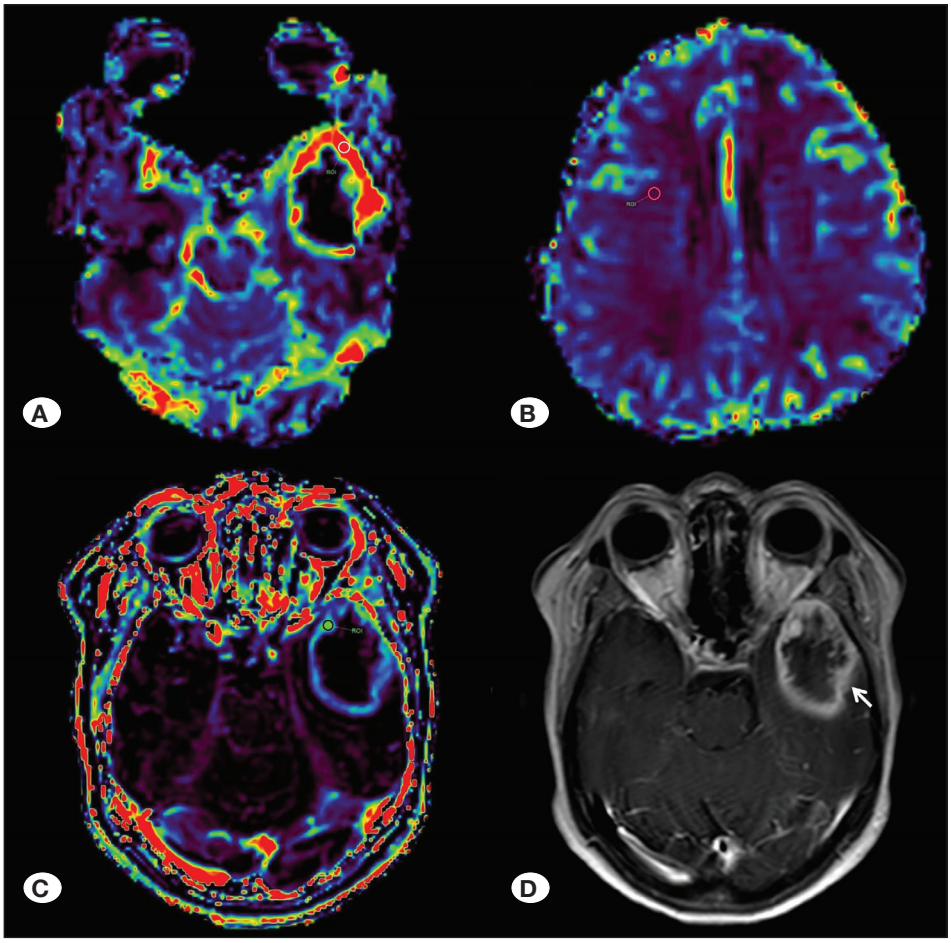

Figure 1: ROI sampling of the regions in a 56-year-old female patient with a diagnosis of IDH wild-type glioblastoma. Colored rCBV map image section from the mostly hyperperfused area **(A)**, and from the contralateral normal-appearing centrum semiovale **(B)**, Ktrans map image section from the region with highest permeability **(C)**, and axial post-contrast T1-weighted image of the same section **(D)** containing the mass which demonstrating peripheral irregular contrast enhancement (arrow) surrounding central necrosis. Similar ROI samplings by use of same technique were made for the remaining perfusion and permeability parameters (not shown). **ROI:** Region of interest, **rCBV:** Relative cerebral blood volume, **IDH:** Isocitrate dehydrogenase.

by dividing a p value of 0.05 by the number of comparisons. Receiver operating characteristic (ROC) curve analysis was performed for perfusion parameters with statistically significant differences between groups of interest. The optimal diagnostic performance cut-off was determined using *Youden's index*. Performance comparison was based on the area under the curve (AUC) of the ROC.

RESULTS

Baseline Characteristics

A total of 40 patients diagnosed with grade 2–4 glioma who underwent DSC- and DCE-MRI examinations before surgery were evaluated for eligibility. Four patients were excluded from the study, as their MRI studies were not assessable due to vascular access problems during contrast administration. Ultimately, 36 patients (22 male and 14 female) met the inclusion criteria. The mean age of the included patients was 49.6 ± 15.6 (range 18–76). The glioma cases mostly comprised IDH wild-type glioblastomas (53%) and IDH mutant oligodendrogliomas with 1p/19q co-deletion (22%). In total, 13 IDH mutant and 23 IDH wild-type gliomas were included. Table I presents detailed histopathological results, including IDH mutation status and WHO grade, for all cases.

Intra- and Inter-Observer Agreement Analysis

Most imaging parameters exhibited good to excellent intra- and inter-observer agreement. The highest intra-observer agreement, with an ICC of 0.993 (95% CI: 0.987–0.997), was observed for Ktrans. Likewise, the highest inter-observer agreement, with an ICC of 0.973 (95% CI: 0.949–0.986), was found for Ve. Table II presents a comprehensive list of ICCs for all perfusion parameters.

IDH Mutation Status Analysis

A corrected statistical significance threshold of 0.00833

Table I: Histopathological Results of 36 Glioma Cases with IDH Mutation Status

Diagnosis	IDH genotype	CNS WHO grade*	Number of cases
Glioblastoma	Wild-type	Grade 4	19
Oligodendroglioma,1p/19q-codeleted	Mutant	Grade 2	5
Oligodendroglioma,1p/19q-codeleted	Mutant	Grade 3	3
Astrocytoma	Mutant	Grade 3	3
Diffuse midline glioma, H3 G34-mutant	Wild-type	Grade 4	3
Astrocytoma	Mutant	Grade 4	1
Astrocytoma	Mutant	Grade 2	1
Adult-type diffuse glioma	Wild-type	Grade 3	1

IDH: *Isocitrate dehydrogenase,* ***CNS:*** *Central nervous system,* ***WHO:*** *World Health Organization.*
**According to 2021, 5th edition.*

Table II: Intraclass Correlation Coefficient Values for All Parameters

Parameter	Agreement	ICC	Lower 95% CI	Upper 95% CI
rCBV	Intra-observer	0.944	0.859	0.974
	Inter-observer	0.889	0.782	0.943
rCBF	Intra-observer	0.899	0.779	0.951
	Inter-observer	0.957	0.915	0.978
Ktrans	Intra-observer	0.993	0.987	0.997
	Inter-observer	0.794	0.572	0.898
Ve	Intra-observer	0.982	0.965	0.991
	Inter-observer	0.973	0.949	0.986
Kep	Intra-observer	0.901	0.816	0.948
	Inter-observer	0.730	0.534	0.852
Vp	Intra-observer	0.000	0.000	0.324
	Inter-observer	0.000	0.000	0.324

ICC: *Intraclass correlation coefficient,* ***CI:*** *Confidence interval,* ***rCBV:*** *Relative cerebral blood volume,* ***rCBF:*** *Relative cerebral blood flow,* ***Ktrans:*** *volume transfer constant,* ***Ve:*** *Extravascular-extracellular volume fraction,* ***Kep:*** *Reflux transfer rate,* ***Vp:*** *Fractional plasma volume*

[0.05/6] was applied according to the *Bonferroni* method to assess statistical differences between IDH mutant and IDH wild-type groups. Two perfusion parameters (rCBV and rCBF) and three permeability parameters (Ktrans, Ve, and Vp) demonstrated a statistically significant difference between the groups based on IDH mutation status (p=0.002 for Vp and p<0.001 for the remaining parameters). Table III and Figure 2 present detailed descriptive statistics and box plots for these significantly different parameters. No significant difference in terms of Kep values was observed between the groups (p=0.123).

Parameters exhibiting statistical significance in the group-based analysis were also subjected to ROC curve analysis. The best diagnostic performance metrics were achieved for Ktrans (cut-off: 0.0727 min^{-1}), with an AUC, sensitivity, specificity, and accuracy of 0.893, 100%, 69.2%, and 88.8%, respectively. The second-best performance metrics were observed for rCBV (cut-off: 5.58), with values of 0.883, 95.7%, 76.9%, and 88.8%, respectively**.** Optimal cut-offs for rCBF, Ve (min^{-1}), and Vp (min^{-1}) were 3.35, 0.6936, and 0.0193, respectively. Table IV shows a comprehensive list of performance metrics of all imaging parameters with optimal cut-offs, and Figure 3 shows their ROC curve.

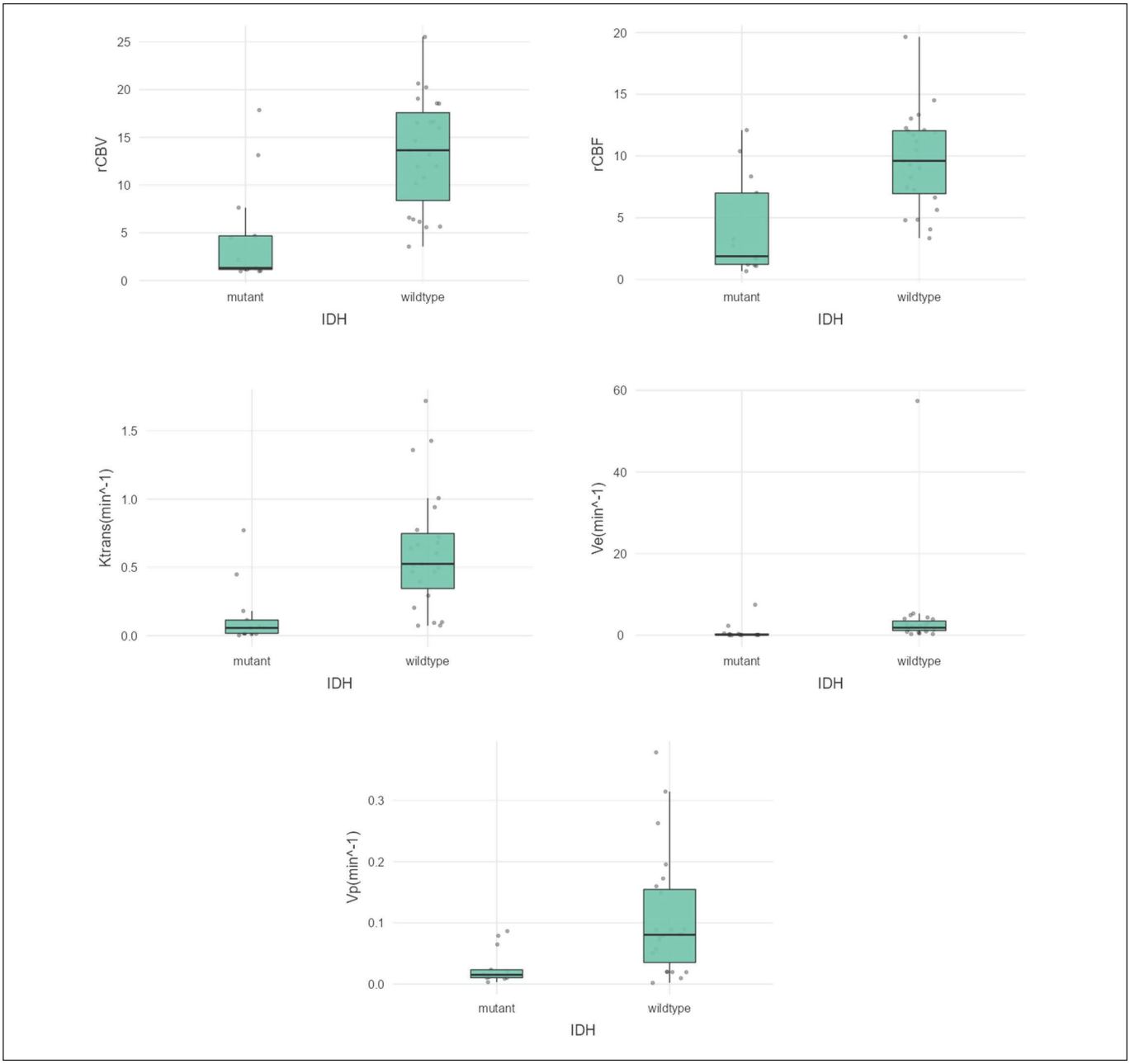

Figure 2: Box plots for statistically significantly different parameters. **rCBV:** Relative cerebral blood volume, **rCBF:** Relative cerebral blood flow, **Ktrans:** Volume transfer constant, **Ve:** Extravascular-extracellular volume fraction, **Vp:** Fractional plasma volume.

Table III: Perfusion Parameters with Descriptive Statistical Results in Terms of IDH Mutation Status

Parameter	IDH	Mean	Median	SD	IQR	Statistic	df	p
rCBV	Mutant	4.457	-	5.380	-	35.000	34	**< 0.001**
	Wild-type	13.422	-	5.869	-			
rCBF	Mutant	4.102	-	3.945	-	44.500	34	**< 0.001**
	Wild-type	9.673	-	3.903	-			
Ktrans (min^{-1})	Mutant	0.136	-	0.226	-	32.000	34	**< 0.001**
	Wild-type	0.620	-	0.440	-			
Ve (min^{-1})	Mutant	0.886	-	2.075	-	40.500	34	**< 0.001**
	Wild-type	4.611	-	11.603	-			
Kep (min^{-1})	Mutant	-	3.065	-	4.045	1.581	34	0.123
	Wild-type	-	2.772	-	1.949			
Vp (min^{-1})	Mutant	0.028	-	0.029	-	57.000	34	**0.002**
	Wild-type	0.108	-	0.100	-			

IDH: *Isocitrate dehydrogenase,* ***rCBV:*** *Relative cerebral blood volume,* ***rCBF:*** *Relative cerebral blood flow,* ***Ktrans:*** *Volume transfer constant,* ***Ve:*** *Extravascular-extracellular volume fraction,* ***Kep:*** *Reflux transfer rate,* ***Vp:*** *Fractional plasma volume,* ***SD:*** *Standard deviation,* ***IQR:*** *Interquantile range,* ***df:*** *Degree of freedom.*

Table IV: Predictive Performance of Each Parameter for Differentiating IDH Mutation Status of Gliomas According to Optimal Cut-Off Values

Parameter	Cut-off	AUC	Accuracy	Sensitivity	Specificity	Youden's index
rCBV	5.58	0.883	88.8%	95.7%	76.9%	0.726
rCBF	3.35	0.851	88.8%	100%	69.2%	0.692
Ktrans (min^{-1})	0.0727	0.893	88.8%	100%	69.2%	0.692
Ve (min^{-1})	0.6936	0.865	86.1%	87.0%	84.6%	0.716
Vp (min^{-1})	0.0193	0.809	80.6%	91.3%	61.5%	0.528

IDH: *Isocitrate dehydrogenase,* ***rCBV:*** *Relative cerebral blood volume,* ***rCBF:*** *Relative cerebral blood flow,* ***Ktrans:*** *Volume transfer constant,* ***Ve:*** *Extravascular-extracellular volume fraction,* ***Vp:*** *Fractional plasma volume,* ***AUC:*** *Area under the receiver operating characteristic curve.*

Tumor Grade Analysis

This study encompassed six cases of grade 2, seven of grade 3, and 23 of grade 4 gliomas. These three groups were initially compared using the Kruskal-Wallis test. The same corrected threshold of 0.00833 [0.05/6] was also applied according to the *Bonferroni* method to assess statistical differences. Similar to IDH analysis results, two perfusion (rCBV and rCBF) and three permeability (Ktrans, Ve, and Vp) parameters exhibited statistically significant differences among the three groups (p=0.006 for Vp and p<0.001 for the remaining parameters). No significant difference was observed for Kep values (p=0.610). For pairwise comparisons, the corrected significance threshold was 0.016. In pairwise comparisons, these five imaging parameters demonstrated significant differences in terms of distinguishing grade 2 from grade 4 gliomas (p<0.001 for all parameters). However, no significant difference was observed in terms of distinguishing grade 2 and 3 gliomas or grade 3 and 4 gliomas.

In an additional analysis, grade 2 gliomas (low-grade) were compared with grade 3 and 4 gliomas (high-grade). Similar to previous analyses, the same five parameters (rCBV, rCBF, Ktrans, Ve, and Vp) demonstrated statistically significant differences between the two groups (p=0.003 for Vp and p<0.001 for the other parameters). No significant difference was observed for Kep values (p=0.116). The best performance metrics were observed for rCBV, rCBF, Ktrans, and Ve, with AUC values exceeding 0.940, sensitivities exceeding 86%, and accuracies exceeding 88%. Table V presents diagnostic performance metrics with the optimal cut-offs for each parameter. Figure 4 shows the results of the ROC curve analysis.

Table V: Predictive Performance of Each Parameter for Differentiating Low (Grade 2) and High Grade (Grade 3 and 4) Gliomas According to Optimal Cut-Off Values

Parameter	Cut-off	AUC	Accuracy	Sensitivity	Specificity	Youden's index
rCBV	4.68	0.972	88.8%	86.7%	100%	0.867
rCBF	3.27	0.972	94.4%	93.3%	100%	0.933
Ktrans (min^{-1})	0.0561	0.947	94.4%	96.7%	83.3%	0.800
Ve (min^{-1})	0.3102	0.950	91.7%	90.0%	100%	0.900
Vp (min^{-1})	0.0234	0.886	75.0%	70.0%	100%	0.700

rCBV: *Relative cerebral blood volume,* ***rCBF:*** *Relative cerebral blood flow,* ***Ktrans:*** *Volume transfer constant,* ***Ve:*** *Extravascular-extracellular volume fraction,* ***Vp:*** *Fractional plasma volume,* ***AUC:*** *Area under the receiver operating characteristic curve.*

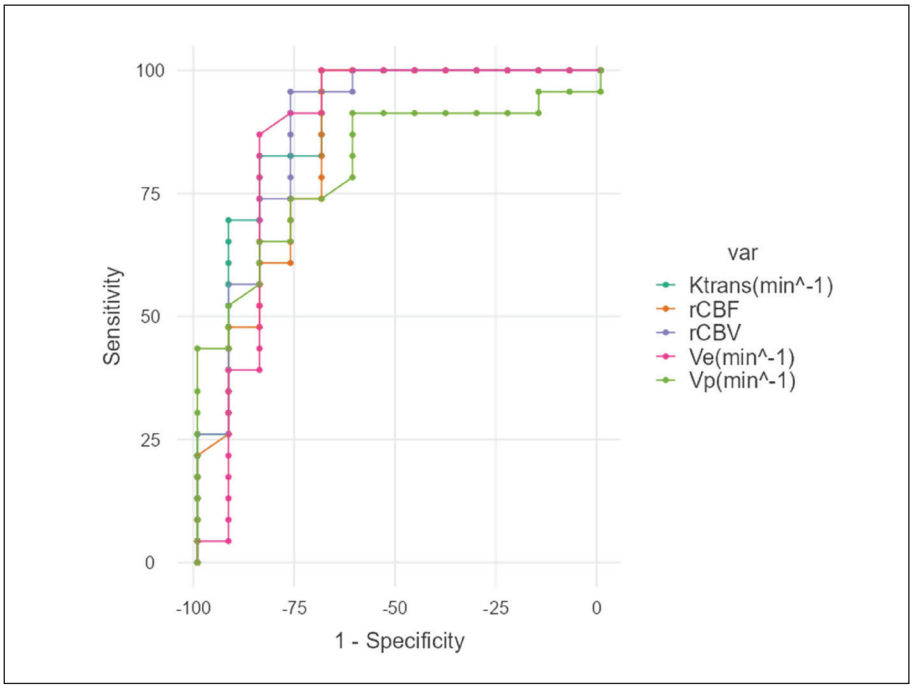

Figure 3: Receiver operating characteristic (ROC) analysis for statistically significantly different parameters in terms of differentiating IDH mutation status.
IDH: isocitrate dehydrogenase.

DISCUSSION

In the current study, we investigated diagnostic performance metrics of perfusion and permeability MRI in determining IDH mutation status and grade in patients with grade 2–4 gliomas. We found that the two imaging parameters acquired from perfusion MRI, rCBV and rCBF, and three imaging parameters acquired from permeability MRI, Ktrans, Ve, and Vp, can non-invasively and correctly distinguish the IDH mutation status and grade of gliomas.

The discovery of the IDH mutations represents a significant milestone in neuro-oncology practice, with significant implications for the classification and prognosis of gliomas (3). It also leads to significant advances in potential new therapeutic approaches for these tumors. The standard treatment process for IDH mutant gliomas typically starts with maximal safe resection. If feasible, surgery is the primary therapeutic intervention and is often followed by a combination of radiotherapy and chemotherapy. However, in some cases, these standard-of-care options offer limited survival benefits and may lead to long-term toxicities, such as cognitive decline, which significantly impact the quality of life of patients and their families (3). Thus, the treatment strategies of IDH mutant gliomas are approaching a more tailored approach. The development of novel and promising treatment strategies continues in this field, including targeting IDH mutations with mIDH inhibitors (ivosidenib, vorasidenib, and olutasidenib), focusing on DNA damage mechanisms (PARP inhibitors), DNA methyltransferase inhibitors (5-azacytidine and decitabine), and immunotherapies (3). We believe these clinical studies, along with non-invasive IDH predictive studies, will soon be critically important, especially in cases where surgery is declined or infeasible. Therefore, we recommend the perfusion and permeability MRI protocol described in this text as a routine examination for patients with suspected glioma. We also believe this method is cost-effective because the imaging protocol

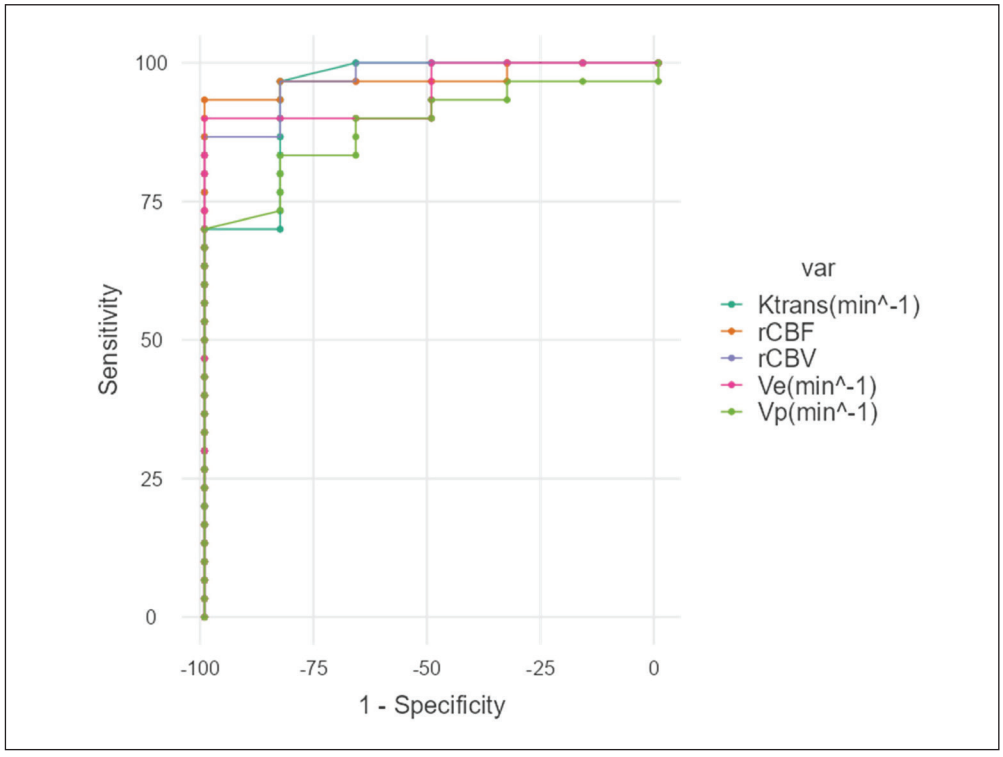

Figure 4: Receiver operating characteristic (ROC) analysis for statistically significantly different parameters in terms of differentiating low- (grade 2) and high-grade (grade 3 and 4) gliomas.

leading to the subsequent detailed analysis is already routinely practiced in glioma cases (1,26).

Several literature studies concern predicting and differentiating the IDH mutation status of gliomas using conventional MRI (12,21,23), diffusion-weighted imaging (24,25), diffusion kurtosis imaging (6,15), amide proton transfer imaging (9), magnetic resonance spectroscopy (19), diffusion tensor imaging (26), and q-sampling imaging (26). Thus far, numerous perfusion-weighted imaging-based studies on the role of perfusion MRI in predicting the grade and IDH genotype of gliomas have also been conducted (1,8,16,20,24). However, only a few of them used DSC and DCE perfusion MRI simultaneously, representing one of the main strengths of the current research. A recent systematic review by van Santwijk et al. provided a valuable insight into the use of perfusion MRI in differentiating the IDH genotype and grade of gliomas (16). A total of 12 studies were included in this meta-analysis; of those, eight used the DSC perfusion technique alone, whereas one used a DCE perfusion technique. However, three of the studies combined the DSC and DCE perfusion techniques. According to this meta-analysis, the data based on DSC perfusion MRI studies showed that the rCBV of IDH mutant gliomas was significantly lower than that of IDH wild-type gliomas. During the differentiation of these two types of glioma, the use of 2.35 as a maximum rCBV threshold value yielded a sensitivity of 100%, specificity of 61%, and AUC of 0.82 (95% CI: 0.66–0.93).

In a recently published permeability MRI-based study, Wu et al. evaluated the diagnostic performance of DCE-MRI parameters for glioma grading in 40 treatment-naive patients (20). Ktrans demonstrated good to excellent accuracy in distinguishing between grades 2 and 3, 3 and 4, and 2 and 4 (AUC = 0.802, 0.801, and 0.971, respectively). In their study, Ve showed good accuracy in distinguishing between grades 3 and 4, as well as 2 and 4 (AUC = 0.874 and 0.899, respectively). In another perfusion MRI-based study including DSC- and DCE-MRI, Ahn et al. assessed the association between perfusion metrics and IDH mutation status in patients with lower-grade gliomas (1). In their study, normalized rCBV values and the ages of individuals were lower in IDH mutant cases than those with IDH wild-type ($p = 0.001$ and $p < 0.001$, respectively). The rCBV was independently associated with the IDH genotype (AUC, 0.817).

Similar to our study, Hilario et al. investigated the diagnostic accuracy of DSC- and DCE-MRI in discriminating the grade and IDH genotype of grade 2–4 gliomas with 49 patients (8). In their study, Ktrans ($p = 0.002$), Vp ($p=0.032$), and Ve ($p<0.001$) showed a significant difference between high- and low-grade diffuse gliomas. The highest AUC was demonstrated by Ktrans (AUC = 0.838) and Ve (AUC = 0.878). The best combination of sensitivity (80%) and specificity (75%) was generated for Ve, with a cut-off of 0.075. A significant difference was also observed in Ktrans values ($p=0.028$) between IDH mutant and IDH wild-type gliomas. Median Ktrans values were 0.13 for IDH mutant and 0.26 for IDH wild-type gliomas. In summary, although significant variations exist in the performance metrics of selected parameters in the studies, it is notable that rCBV and Ktrans are conspicuous in most of them, as in our study. Given recent revisions and updates in the grade and molecular characteristics of gliomas, as well as the lack of consensus regarding which parameters and cut-offs should be used, we believe new studies with larger sample sizes

should be conducted on predicting glioma subtypes and molecular features.

This study has the following limitations: its small sample size, retrospective nature, and single institution. Another limitation of this study was the inclusion of gliomas with various subtypes and grades. Given the limited sample size, different IDH subtypes were not considered (i.e., IDH1 and IDH2). We intend to extend the analysis by including additional cases. ROIs were generated manually in this study. While the ICC estimates for the parameters indicated high reproducibility, this process must be automated to further enhance reproducibility, reduce reader dependency, and decrease the time required for clinical applications. Finally, the analysis of the perfusion parameters is limited to univariate statistics because multivariate analysis with a small number of patients might have risked overfitting. However, we performed the univariate analysis under appropriate multiplicity corrections in every stage to mitigate the risk of false discovery.

CONCLUSION

In conclusion, parameters acquired from perfusion and permeability MRI may be able to non-invasively correctly distinguish the IDH mutation status and grade of gliomas. Our results support the literature, which contains a few studies simultaneously including these two advanced MRI techniques. Further studies with larger sample sizes are warranted to clarify the optimal cut-offs.

Declarations

Funding: The authors declare that no funds, grants, or other support were received during the preparation of this manuscript.

Availability of data and materials: The datasets generated during and/or analysed during the current study are available from the corresponding author on reasonable request.

Disclosure: The Authors declare that there is no conflict of interest.

AUTHORSHIP CONTRIBUTION

Study conception and design: SY, BK

Data collection: SY, MK, MSO

Analysis and interpretation of results: BK, SY

Draft manuscript preparation: SY, BK, SM

All authors (SY, MK, MSO, SM, BK) reviewed the results and approved the final version of the manuscript.

REFERENCES

1. Ahn SH, Ahn SS, Park YW, Park CJ, Lee SK: Association of dynamic susceptibility contrast- and dynamic contrast-enhanced magnetic resonance imaging parameters with molecular marker status in lower-grade gliomas: A retrospective study. Neuroradiol J 36:49-58, 2023. https://doi.org/10.1177/19714009221098369
2. Alksas A, Shehata M, Atef H, Sherif F, Alghamdi NS, Ghazal M, Abdel Fattah S, El-Serougy LG, El-Baz A: A novel system for precise grading of glioma. Bioengineering (Basel) 9:532, 2022. https://doi.org/10.3390/bioengineering9100532
3. Alshiekh Nasany R, de la Fuente MI: Therapies for IDH-mutant gliomas. Curr Neurol Neurosci Rep 23225-233, 2023. https://doi.org/10.1007/s11910-023-01265-3
4. Bi J, Chowdhry S, Wu S, Zhang W, Masui K, Mischel PS: Altered cellular metabolism in gliomas - an emerging landscape of actionable co-dependency targets. Nat Rev Cancer 20:57-70, 2020. https://doi.org/10.1038/s41568-019-0226-5
5. Boxerman JL, Quarles CC, Hu LS, Erickson BJ, Gerstner ER, Smits M, Kaufmann TJ, Barboriak DP, Huang RH, Wick W, Weller M, Galanis E, Kalpathy-Cramer J, Shankar L, Jacobs P, Chung C, van den Bent MJ, Chang S, Al Yung WK, Cloughesy TF, Wen PY, Gilbert MR, Rosen BR, Ellingson BM, Schmainda KM; Jumpstarting Brain Tumor Drug Development Coalition Imaging Standardization Steering Committee: Consensus recommendations for a dynamic susceptibility contrast MRI protocol for use in high-grade gliomas. Neuro Oncol 22:1262-1275, 2020. https://doi.org/10.1093/neuonc/noaa141
6. Chawla S, Krejza J, Vossough A, Zhang Y, Kapoor GS, Wang S, O'Rourke DM, Melhem ER, Poptani H: Differentiation between oligodendroglioma genotypes using dynamic susceptibility contrast perfusion-weighted imaging and proton MR spectroscopy. AJNR Am J Neuroradiol 34:1542-1549, 2013. https://doi.org/10.3174/ajnr.A3384
7. Ge X, Wang M, Ma H, Zhu K, Wei X, Li M, Zhai X, Shen Y, Huang X, Hou M, Liu W, Wang M, Wang X: Investigated diagnostic value of synthetic relaxometry, three-dimensional pseudo-continuous arterial spin labelling and diffusion-weighted imaging in the grading of glioma. Magn Reson Imaging 86:20-27, 2022. https://doi.org/10.1016/j.mri.2021.11.006
8. Hilario A, Hernandez-Lain A, Sepulveda JM, Lagares A, Perez-Nuñez A, Ramos A: Perfusion MRI grading diffuse gliomas: Impact of permeability parameters on molecular biomarkers and survival. Neurocirugia (Astur: Engl Ed) 30:11-18, 2019. https://doi.org/10.1016/j.neucir.2018.06.004
9. Jiang S, Zou T, Eberhart CG, Villalobos MAV, Heo HY, Zhang Y, Wang Y, Wang X, Yu H, Du Y, van Zijl PCM, Wen Z, Zhou J: Predicting IDH mutation status in grade II gliomas using amide proton transfer-weighted (APTw) MRI. Magn Reson Med 78:1100-1109, 2017. https://doi.org/10.1002/mrm.26820
10. Koo TK, Li MY: A guideline of selecting and reporting intraclass correlation coefficients for reliability research. J Chiropr Med 15:155-163, 2016. https://doi.org/10.1016/j.jcm.2016.02.012
11. Louis DN, Perry A, Wesseling P, Brat DJ, Cree IA, Figarella-Branger D, Hawkins C, Ng HK, Pfister SM, Reifenberger G, Soffietti R, von Deimling A, Ellison DW: The 2021 WHO classification of tumors of the central nervous system: A summary. Neuro Oncol 23:1231-1251, 2021. https://doi.org/10.1093/neuonc/noab106
12. Qi S, Yu L, Li H, Ou Y, Qiu X, Ding Y, Han H, Zhang X: Isocitrate dehydrogenase mutation is associated with tumor location and magnetic resonance imaging characteristics in astrocytic neoplasms. Oncol Lett 7:1895-1902, 2014. https://doi.org/10.3892/ol.2014.2013
13. Shrout PE, Fleiss JL: Intraclass correlations: Uses in assessing rater reliability. Psychol Bull 86:420-428, 1979. https://doi.org/10.1037//0033-2909.86.2.420

14. Suh CH, Kim HS, Jung SC, Choi CG, Kim SJ: Imaging prediction of isocitrate dehydrogenase (IDH) mutation in patients with glioma: A systemic review and meta-analysis. Eur Radiol 29:745-758, 2019. https://doi.org/10.1007/s00330-018-5608-7
15. Tan Y, Zhang H, Wang X, Qin J, Wang L, Yang G, Yan H: Comparing the value of DKI and DTI in detecting isocitrate dehydrogenase genotype of astrocytomas. Clin Radiol 74:314-320, 2019. https://doi.org/10.1016/j.crad.2018.12.004
16. van Santwijk L, Kouwenberg V, Meijer F, Smits M, Henssen D: A systematic review and meta-analysis on the differentiation of glioma grade and mutational status by use of perfusion-based magnetic resonance imaging. Insights Imaging 13:102, 2022. https://doi.org/10.1186/s13244-022-01230-7
17. Villanueva-Meyer JE, Wood MD, Choi BS, Mabray MC, Butowski NA, Tihan T, Cha S: MRI features and IDH mutational status of grade II diffuse gliomas: Impact on diagnosis and prognosis. AJR Am J Roentgenol 210:621-628, 2018. https://doi.org/10.2214/AJR.17.18457
18. Weller M, van den Bent M, Tonn JC, Stupp R, Preusser M, Cohen-Jonathan-Moyal E, Henriksson R, Le Rhun E, Balana C, Chinot O, Bendszus M, Reijneveld JC, Dhermain F, French P, Marosi C, Watts C, Oberg I, Pilkington G, Baumert BG, Taphoorn MJB, Hegi M, Westphal M, Reifenberger G, Soffietti R, Wick W; European Association for Neuro-Oncology (EANO) Task Force on Gliomas: European Association for Neuro-Oncology (EANO) guideline on the diagnosis and treatment of adult astrocytic and oligodendroglial gliomas. Lancet Oncol 18:e315-e329, 2017. https://doi.org/10.1016/S1470-2045(17)30194-8
19. Whitmore RG, Krejza J, Kapoor GS, Huse J, Woo JH, Bloom S, Lopinto J, Wolf RL, Judy K, Rosenfeld MR, Biegel JA, Melhem ER, O'Rourke DM: Prediction of oligodendroglial tumor subtype and grade using perfusion weighted magnetic resonance imaging. J Neurosurg 107:600-609, 2007. https://doi.org/10.3171/JNS-07/09/0600
20. Wu J, Liang Z, Deng X, Xi Y, Feng X, Yao Z, Shu Z, Xie Q: Glioma grade discrimination with dynamic contrast-enhanced MRI: An accurate analysis based on MRI guided stereotactic biopsy. Magn Reson Imaging 99:91-97, 2023. https://doi.org/10.1016/j.mri.2023.02.003
21. Wang YY, Wang K, Li SW, Wang JF, Ma J, Jiang T, Dai JP: Patterns of tumor contrast enhancement predict the prognosis of anaplastic gliomas with IDH1 mutation. AJNR Am J Neuroradiol 36:2023-2029, 2015. https://doi.org/10.3174/ajnr.A4407
22. Xiao A, Shen B, Shi X, Zhang Z, Zhang Z, Tian J, Ji N, Hu Z: Intraoperative glioma grading using neural architecture search and multi-modal imaging. IEEE Trans Med Imaging 41:2570-2581, 2022. https://doi.org/10.1109/TMI.2022.3166129
23. Xing Z, Zhang H, She D, Lin Y, Zhou X, Zeng Z, Cao D: IDH genotypes differentiation in glioblastomas using DWI and DSC-PWI in the enhancing and peri-enhancing region. Acta Radiol 60:1663-1672, 2019. https://doi.org/10.1177/0284185119842288
24. Xing Z, Yang X, She D, Lin Y, Zhang Y, Cao D: Noninvasive assessment of IDH mutational status in World Health Organization Grade II and III Astrocytomas using DWI and DSC-PWI combined with conventional MR imaging. AJNR Am J Neuroradiol 38:1138-1144, 2017. https://doi.org/10.3174/ajnr.A5171
25. Xiong J, Tan WL, Pan JW, Wang Y, Yin B, Zhang J, Geng DY: Detecting isocitrate dehydrogenase gene mutations in oligodendroglial tumors using diffusion tensor imaging metrics and their correlations with proliferation and microvascular density. J Magn Reson Imaging 43:45-54, 2016. https://doi.org/10.1002/jmri.24958
26. Yuzkan S, Mutlu S, Han M, Akkurt TS, Sencan F, Kusku Cabuk F, Gunaldi O, Tugcu B, Kocak B: Predicting isocitrate dehydrogenase mutation status of grade 2-4 gliomas with diffusion tensor imaging (DTI) parameters derived from model-based DTI and model-free Q-sampling imaging reconstructions. World Neurosurg 177:e580-e592, 2023. https://doi.org/10.1016/j.wneu.2023.06.099
27. Yuzkan S, Mutlu S, Karagulle M, Sam Ozdemir M, Ozgul H, Arikan MA, Kocak B: Reproducibility of rCBV in glioblastomas using T2*-weighted perfusion MRI: An evaluation of sampling, normalization, and experience. Diagn Interv Radiol 30:124-134, 2024. https://doi.org/10.4274/dir.2023.232442